

# MOCVD of hard metallurgical coatings: Examples in the Cr–C–N system

**F. Maury**

CIRIMAT, CNRS, ENSIACET, 118 Route de Narbonne, 31077 Toulouse Cedex 4, France

## **Abstract**

All individual phases of the ternary Cr–C–N system including stable and metastable ones can be deposited at low temperature by metalorganic chemical vapor deposition (MOCVD). These growth processes are mainly based on the use of bis(benzene)chromium as chromium source and various co-reactives. Then, from a good control of the reactive gas phase, it is possible to combine these MOCVD processes to grow in the same reactor protective coatings designed with a complex architecture based on polyphased, nanostructured or multilayer structure which exhibit enhanced properties. These deposition processes are described and the main features of the coatings are discussed.

**Keywords:** MOCVD; Metalorganic precursors; Chromium nitrides; Chromium carbides; Hard coatings

1. Introduction
  2. Experimental
  3. Growth using  $\text{Cr}(\text{C}_6\text{H}_6)_2/\text{H}_2$
  4. Growth using  $\text{Cr}(\text{C}_6\text{H}_6)_2/\text{C}_6\text{Cl}_6$
  5. Growth using  $\text{Cr}(\text{C}_6\text{H}_6)_2/\text{NH}_3$
  6. Growth using  $\text{Cr}(\text{C}_6\text{H}_6)_2/\text{C}_6\text{Cl}_6/\text{NH}_3$
  7. Growth using the single-source  $\text{Cr}(\text{NET}_2)_4$
  8. Conclusions
- Acknowledgements  
References

## **1. Introduction**

The use of metalorganic compounds as molecular precursors in chemical vapor deposition process (MOCVD) allows on one hand a significant decrease of the deposition temperatures and, on the other hand, considerably extends the type of materials which can be deposited, thus offering new routes for advanced coating materials. As a result, MOCVD, which is a well-known technique in microelectronic area, offers promising prospects for applications of hard metallurgical coatings. The protective coatings make very significant progress, thanks to complex architectures designed to optimize the properties by including the behavior of the interface with the support and that of external surface with the environment [1]. From this point of view the ternary systems are particularly interesting because they offer a high flexibility in designing the microstructure and

architecture of the coatings [2]. The system Cr–C–N was selected both to illustrate the good potentiality of MOCVD processes in this applicability and because it has a great interest.

Indeed, Ti-based materials are the most employed hard metallurgical coatings in the field of abrasive wear protection. However, chromium nitrides are recommended as wear resistant coatings under hostile atmosphere because they combine resistance to wear and to chemical attack by various agents even at high temperature. Compared to TiN, CrN has a better resistance to oxidation at high temperature [3] and to corrosion in different environments [4] and [5]. Moreover, it exhibits a slightly lower friction coefficient [4], [6] and [7] and comparable adherence [8]. Thereby, the tribological performance of CrN is better than TiN under dry [7] and [8] and lubricated [8] and [9] conditions. CrN also has a better resistance to Cl-attack than (Ti,Al)N [10]. These data strongly increase the interest for CrN as wear protective coating in applications, such as hot forming, plastic molding, drawing, etc. ... In addition, CrN has been proposed as solar selective absorber [11] and it could find applications in microelectronics as barrier against Cu diffusion [12] and hardmask for precise X-ray lithography [13].

Moreover, Cr<sub>2</sub>N and CrN exhibit different properties, which allows tailoring of the properties of dual phase coatings in a wide range depending on the proportion of each phase. For instance, Cr<sub>2</sub>N is more covalent than CrN, and therefore, it exhibits a higher hardness [6]. Cr<sub>2</sub>N layers exhibit frequently lower residual stresses than CrN [14] but the cubic phase is more resistant in sulfuric acid solutions than the hexagonal one [15] and has a better oxidation resistance at high temperature than PVD bi-phased Cr:Cr<sub>2</sub>N coatings [16]. On the other hand, it is possible in PVD dual phase Cr<sub>2</sub>N:CrN coatings to control the residual stresses of the films from tensile to compressive by adjusting the volume fraction of each phase [14].

In addition to the chromium nitrides phases, the ternary Cr–N–C system exhibits three stable carbides, a low solubility of carbon in \*Cr and a large solid solution Cr<sub>2</sub>(N,C) (Fig. 1), as well as a metastable phase Cr<sub>3</sub>(C<sub>0.8</sub>N<sub>0.2</sub>)<sub>2</sub>. Due to the existence of all these phases, chromium nitride coatings are more sensitive to minor changes of the local growth conditions in the deposition chamber compared to TiN. By contrast their properties can be tailored in a wider range than those of other ternary systems by depositing a particular single phase or dual phase coatings with a controlled composition.

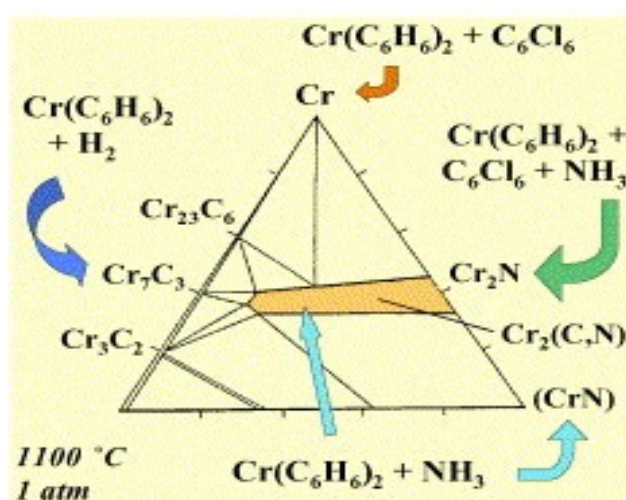


Fig. 1. Ternary section (1100 °C; 1 atm) showing all the stable phases of the Cr–N–C system and

MOCVD processes used for their deposition (the processes are symbolized by the reactive mixtures).

We have investigated MOCVD routes for the low temperature deposition of the individual phases of the Cr–N–C system using mixtures of bis(benzene)chromium, BBCr, as starting material and various co-reactives. The processes are summarized in [Fig. 1](#) and are briefly reviewed in this paper.

## 2. Experimental

Deposition experiments were carried out in a horizontal, hot-wall quartz CVD reactor 2.5 cm in diameter with an isothermal zone of ca. 20 cm excepted otherwise specified. The gas streams (He, H<sub>2</sub>, Ar, NH<sub>3</sub>, all electronic grade) were monitored using mass flowmeters and the total pressure was automatically controlled. The molecular precursors, Cr(C<sub>6</sub>H<sub>6</sub>)<sub>2</sub> and C<sub>6</sub>Cl<sub>6</sub>, were handled in a glove box and put into sublimation vessels thermostated at 95 and 20 °C, respectively. Details on the experimental conditions are given in the cited references. A set of representative MOCVD runs is reported in [Table 1](#).

Table 1.

	BBCr:C <sub>6</sub> Cl <sub>6</sub>	BBCr:NH <sub>3</sub>		BBCr:NH <sub>3</sub> :C <sub>6</sub> Cl <sub>6</sub>		
	D2 <sup>a</sup>	S4 <sup>a</sup>	S1 <sup>a</sup>	D4 <sup>a</sup>	D5 <sup>a</sup>	D6 <sup>a</sup>
Growth temperature (°C)	350	527	527	500	450	450
Total pressure (kPa)	0.08	0.5	0.5	1.33	1.33	1.33
He flow rate (sccm)	200	150	150	200	200	200
H <sub>2</sub> flow rate (sccm)	100	0	0	120	120	120
NH <sub>3</sub> flow rate (sccm)	0	17	75	180	180	200
x[Cr(C <sub>6</sub> H <sub>6</sub> ) <sub>2</sub> ]	6.3 × 10 <sup>-3</sup>	5 × 10 <sup>-3</sup>	1.4 × 10 <sup>-3</sup>	1.9 × 10 <sup>-4</sup>	3.6 × 10 <sup>-4</sup>	2.6 × 10 <sup>-4</sup>
C <sub>6</sub> Cl <sub>6</sub> :Cr(C <sub>6</sub> H <sub>6</sub> ) <sub>2</sub>	0.14	0	0	0	0.11	0.14
NH <sub>3</sub> :Cr(C <sub>6</sub> H <sub>6</sub> ) <sub>2</sub>	0	20	240	1892	986	1508
Growth rate (μm/h)	~3	3	~10	~0.25	~0.25	~0.25

<sup>a</sup> Run.

### 3. Growth using $\text{Cr}(\text{C}_6\text{H}_6)_2/\text{H}_2$

A thermodynamic analysis was performed in the Cr–C–H–He system to simulate the use of the reactive gas mixture  $\text{Cr}(\text{C}_6\text{H}_6)_2/\text{H}_2$  [17]. The calculations have shown that it is possible to go through the different regions of the Cr–C phase diagram, from the C-rich biphased  $\text{Cr}_3\text{C}_2 + \text{C}$  region to pure Cr metal, by decreasing the deposition temperature, working under atmospheric pressure and using a very low mole fraction of  $\text{Cr}(\text{C}_6\text{H}_6)_2$  in  $\text{H}_2$  as illustrated in Fig. 2. It can be noted that the requirement of low BBCr mole fraction is a disadvantage for optimizing the growth rate. The trend predicted by thermodynamic modeling is consistent with experiment data but an overestimation of the theoretical C content was found. It was assumed that BBCr undergoes rapid and partial gas phase decomposition, which releases  $\text{C}_6\text{H}_6$  molecules that do not participate to the growth mechanism. Partial equilibrium calculations starting with the fictive nutrient species  $\text{Cr}(\text{C}_6\text{H}_6)_x$  are in good agreement with experimental results for  $x = 0.2$  instead of 2. This value of 0.2 is consistent with a model considering the C incorporation is controlled by surface adsorption of benzene molecules [17]. As a result, a better way to reduce or suppress C from the coatings is to block adsorption of benzene and, subsequently, prevent its heterogeneous decomposition.

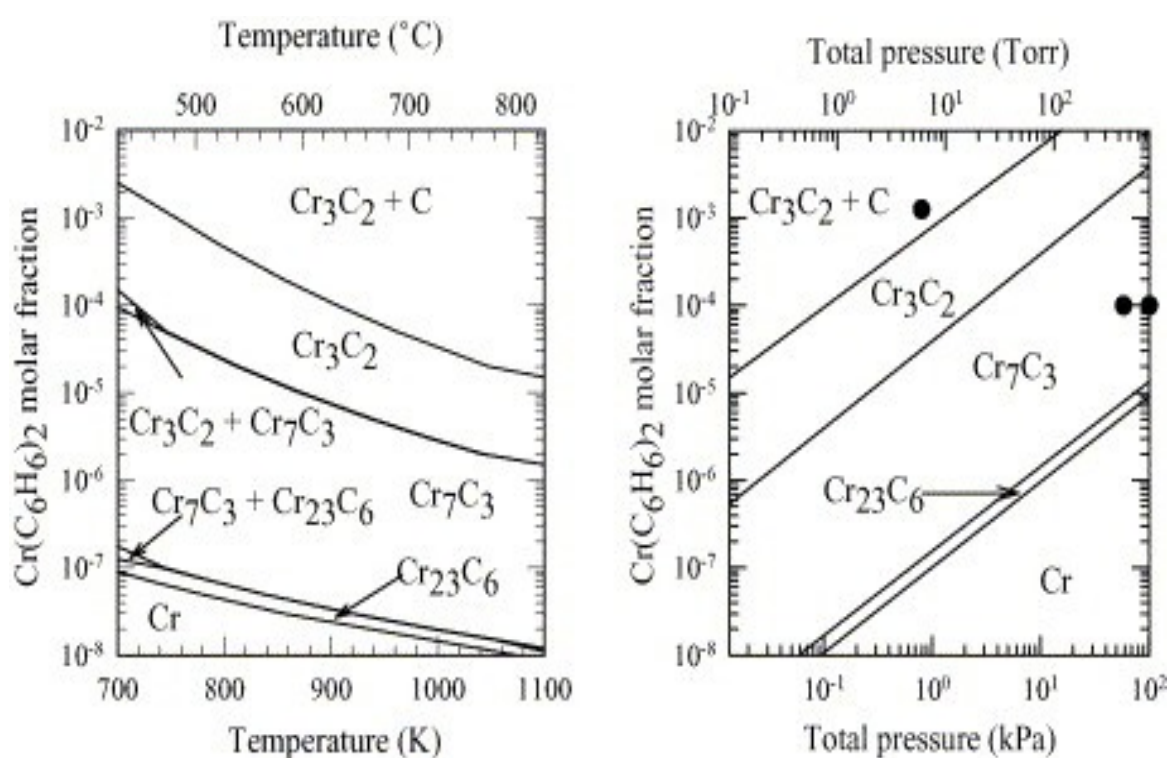


Fig. 2. Deposition diagrams in the Cr–C–H system calculated as a function of the mole fraction of  $\text{Cr}(\text{C}_6\text{H}_6)_2$  in  $\text{H}_2$  ambient and (a) the deposition temperature ( $P = 0.4$  kPa) and (b) the total pressure ( $T = 823$  K). The black points correspond to experiments reported in [17] (reproduced with the permission of The Electrochemical Society, Inc.).

#### 4. Growth using $\text{Cr}(\text{C}_6\text{H}_6)_2/\text{C}_6\text{Cl}_6$

The deposition conditions of the previous section are not useful for large-scale applications since they lead to a poor uniformity and a low growth rate of the metal thin films. Hard Cr metal coatings (and not of chromium carbide) are more conveniently deposited at low temperature (350 °C) by addition of small amounts of  $\text{C}_6\text{Cl}_6$  (4–9%) to the input gas phase. Interestingly, they exhibit a very high hardness ( $\sim 21$  GPa) and a good adhesion to steel substrates. This MOCVD process operates under low pressure and the use of  $\text{H}_2$  is not required unlike in the first route.

A growth mechanism supported by on-line mass spectrometry (MS) analyses was investigated [18]. The  $\text{C}_6\text{Cl}_6$  molecules likely acts directly on surface reactions by favoring a reaction pathway which is not expected on the basis of thermodynamic calculations.  $\text{C}_6\text{H}_6$  and  $\text{H}_2$  are the major gaseous by-products formed during MOCVD using  $\text{Cr}(\text{C}_6\text{H}_6)_2$ . In the temperature range of the growth (300–700 °C), free  $\text{C}_6\text{H}_6$  molecules are not pyrolyzed in the gas phase and, therefore, the intensity ratio  $I(2)/I(78)$  analyzed by MS should be constant (this corresponds to the  $\text{H}_2:\text{C}_6\text{H}_6$  ratio). In fact, it slightly decreases by increasing the temperature likely because a better diffusion in the sampling system toward the mass spectrometer occurs at high temperatures. The same behavior is observed in this temperature range using  $\text{Cr}(\text{C}_6\text{H}_6)_2/\text{C}_6\text{Cl}_6/\text{He}$ , indicating that  $\text{H}_2$  is not significantly formed from this reactive gas mixture (Fig. 3). In this last process, benzene ligands are released without further decomposition and, subsequently, Cr metal is deposited. On the contrary, when using  $\text{Cr}(\text{C}_6\text{H}_6)_2/\text{He}$  as input gas mixture, the continuous increase of the intensity ratio  $I(2)/I(78)$  with the temperature gives evidence for  $\text{H}_2$  formation in the temperature range of the deposition, originating from heterogeneous dehydrogenation of  $\text{C}_6\text{H}_6$  and resulting in the growth of chromium carbides (Fig. 3).

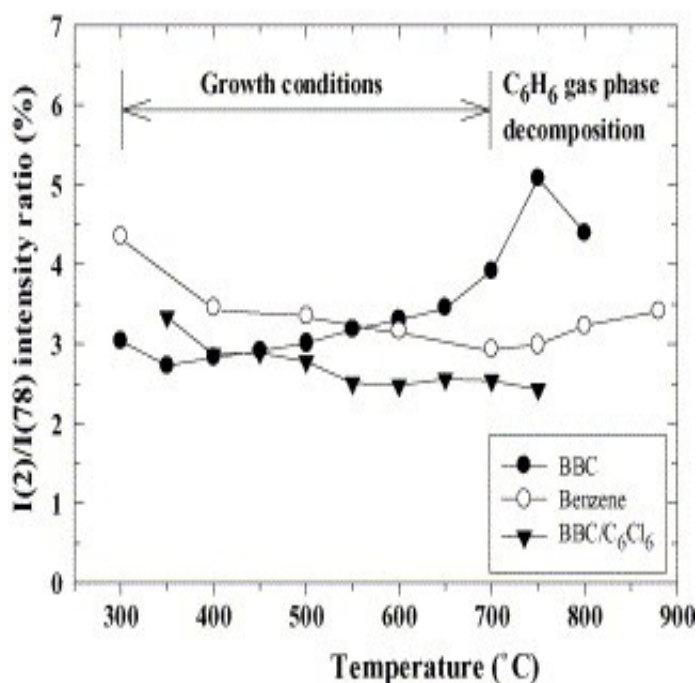


Fig. 3. Variation with the temperature of the intensity ratio of the ion fragments  $m/q = 2$  ( $H_2$ ) and 78 (benzene) using  $C_6H_6$  ( $\circ$ ),  $Cr(C_6H_6)_2$  ( $\bullet$ ) and  $Cr(C_6H_6)_2/C_6Cl_6$  ( $\blacktriangledown$ ) as input gas phase (carrier gas He;  $P = 0.8$  kPa;  $x_{BBCr} = 2.1 \times 10^{-3}$ ;  $C_6Cl_6/BBCr = 4.4$ ).

It was proposed in the previous section that the adsorption of  $C_6H_6$  played a major role in the growth mechanism using  $BBCr/H_2$ . Here, it is assumed that  $C_6Cl_6$  molecules displace adsorbed benzene as gaseous  $C_6H_6$  molecules, block their adsorption sites, and then prevent their heterogeneous dehydrogenation and the subsequent C incorporation into the layer.

### 5. Growth using $Cr(C_6H_6)_2/NH_3$

The cubic phase CrN has been deposited under low pressure using  $Cr(C_6H_6)_2$  as Cr source and  $NH_3$  [19]. The MOCVD conditions are reported in [Table 1](#). The layers grown at  $T \leq 450$  °C using the reactive gas mixture  $Cr(C_6H_6)_2/NH_3$  are XRD amorphous. They exhibit a crystalline structure when they are grown at 527 °C. For a large excess of  $NH_3$ , single phase CrN coatings are formed with a very low C incorporation in agreement with the fact that C is not soluble in this cubic phase (run S1 and D4). The presence of  $H_2$  does not change significantly the composition and the structure of these films ([Table 2](#)).

---

---

Table 2.

Run	Composition (EPMA)	Structure (XRD)			Properties		
		Phase	$T_{\text{CrII}(111)}$	$D_{\text{CrII}(111)}$ (nm)	HK, 25 g (GPa)	$\sigma_{\text{th}}$ (GPa)	$\sigma_{\text{R}}$ (GPa)
D2	Cr <sub>0.96</sub> C <sub>0.04</sub>	bcc-Cr	–	–	19.0 <sup>a</sup>	-0.84	-0.73
S4	Cr <sub>0.64</sub> N <sub>0.17</sub> C <sub>0.19</sub>	$\xi$ -Cr <sub>2</sub> (N,C)	–	–	14.7 <sup>b</sup>	–	–
S1	Cr <sub>0.48</sub> N <sub>0.49</sub> C <sub>0.03</sub>	CrN	–	–	18.6 <sup>b</sup>	–	–
D4	Cr <sub>0.55</sub> N <sub>0.43</sub> C <sub>0.02</sub>	CrN	1.4	7 ± 2	14.3	–	–
D5	Cr <sub>0.58</sub> N <sub>0.38</sub> C <sub>0.04</sub>	Cr <sub>2</sub> N + CrN	1.5	19 ± 6	14.1	-1.0	-0.13
D6	Cr <sub>0.53</sub> N <sub>0.42</sub> C <sub>0.05</sub>	CrN (+ tr. Cr <sub>2</sub> N)	1.0	10 ± 4	12.7	-1.0	+0.31

<sup>a</sup> Nanohardness measured using indentation loads in the range 5–30 mN.

<sup>b</sup> Vickers microhardness measured using a test load of 50 g.

The Cr–N–C system exhibits an extended ternary solid solution Cr<sub>2</sub>(N,C), which exhibits the hexagonal  $\beta$ -Cr<sub>2</sub>N structure for C content lower than 15 at.% ( $\epsilon$ -Fe<sub>2</sub>N-type structure), and the orthorhombic  $\xi$ -Fe<sub>2</sub>N-type structure for C content in the range 15–22 at.% [20]. With this dual-source MOCVD process (BBCr/NH<sub>3</sub> mixture), CrN is obtained at high NH<sub>3</sub> partial pressure and decreasing NH<sub>3</sub> concentration leads to the growth of the orthorhombic solid solution Cr<sub>2</sub>(N,C) rather than that of the hexagonal nitride Cr<sub>2</sub>N (run S4). Thus, due to the high concentration of organic species in the gas phase originating from the metalorganic precursor and the high solubility of C in Cr<sub>2</sub>N, it is not possible to go through the Cr<sub>2</sub>(N,C) solid solution toward the N-rich region. As a result, the composition of the solid solution is in the C-rich region ( $\sim$ 19 at.%) and it exhibits usually the orthorhombic  $\xi$ -Fe<sub>2</sub>N-type structure [21].

## 6. Growth using Cr(C<sub>6</sub>H<sub>6</sub>)<sub>2</sub>/C<sub>6</sub>Cl<sub>6</sub>/NH<sub>3</sub>

In this triple-source MOCVD process, the reduction of C incorporation into the layers is noteworthy (Table 2). The C content is typically 4 at.% (runs D5 and D6). Furthermore, the films exhibit a good crystallinity at 450 °C whereas they are amorphous in absence of C<sub>6</sub>Cl<sub>6</sub>. This chlorinated additive prevents the C incorporation and facilitates the crystal growth of chromium nitride coatings. XRD analyses reveal a biphased structure constituted of the cubic CrN and the hexagonal  $\beta$ -Cr<sub>2</sub>N phases. Their proportion strongly depends on the mole fraction ratio NH<sub>3</sub>:BBCr [21]. For instance, the ratio

$\text{Cr}_2\text{N}:\text{CrN}$  is close to 50:50 in the sample D5 while CrN becomes the major phase by increasing the  $\text{NH}_3:\text{BBCr}$  ratio as in the run D6 (Fig. 4).

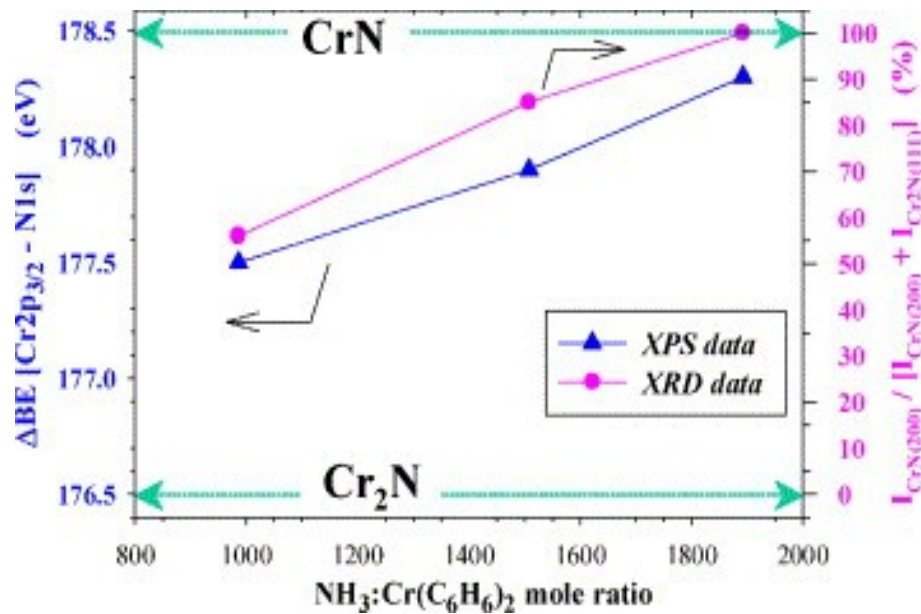


Fig. 4. Influence of the  $\text{NH}_3:\text{BBCr}$  ratio on the proportion of each phase in dual phase  $\text{Cr}_2\text{N}:\text{CrN}$  coatings. Data originate from XPS (binding energy difference between Cr  $2p_{3/2}$  and N  $1s$ ,  $\Delta\text{BE}$ ) and XRD (relative intensity of  $\text{Cr}_2\text{N}(1\ 1\ 1)$  and  $\text{CrN}(2\ 0\ 0)$  peaks).

The presence of small amount of C into the layers was confirmed by XPS analyses. Furthermore, the films are not contaminated by chlorine. The carbon is mainly in the form of free C with a C  $1s$  core level at 284.9 eV ( $\geq 80\%$  of the total C) in CrN film (D4), while a predominant contribution of a carbidic form ( $\sim 60\%$  of the total C) was observed at 282.5 eV in dual phase  $\text{Cr}_2\text{N}:\text{CrN}$  coatings. This is in agreement with the high solubility of C into  $\text{Cr}_2\text{N}$ . Due to the higher ionicity of CrN compared to  $\text{Cr}_2\text{N}$ , a significant difference of binding energy  $\Delta\text{BE}$  is expected between the Cr  $2p_{3/2}$  and N  $1s$  core levels: 178.5 and 176.5 eV for CrN and  $\text{Cr}_2\text{N}$ , respectively [22]. The proportion of each phase determined from  $\Delta\text{BE}$  is in good agreement with the XRD data (Fig. 4).

The CrN films exhibit a relatively high Knoop hardness (14 GPa) compared to the 4.9 GPa of the substrate. The microhardness reaches 24 GPa for a load of 10 g for the CrN sample D4. Excepted for the bcc-type Cr coating (D2), which exhibits a very high hardness for this type of films [18], there is no significant difference in the hardness values of the nitride samples prepared in this study.

The residual stresses  $\sigma_R$  determined from the curvature change of the samples before and after deposition reveal that the bcc-type Cr sample exhibits a compressive stress ( $-0.73$  GPa) of the same order than the thermal stresses ( $\sigma_{th} = -0.81$  GPa) indicating that the intrinsic stresses ( $\sigma_R - \sigma_{th}$ ) are almost negligible. The residual stresses of the dual phase coatings (D5, D6) are relatively low. They are slightly compressive for the 50:50  $\text{Cr}_2\text{N}:\text{CrN}$  coatings ( $-0.13$  GPa) and they change to tensile ( $+0.31$  GPa) for the CrN-rich coatings (D6). Interestingly, a compressive-to-tensile transition likely



occurs for a particular volume fraction of each phase. This was also observed for similar PVD dual phase coatings for which it was possible to adjust  $\sigma_R$  by controlling the volume fraction of the phases [14]. This result is noteworthy because there is a need for low-stress chromium nitride films for instance as hardmask [13].

## 7. Growth using the single-source $\text{Cr}(\text{NEt}_2)_4$

Single-phased and nanocrystalline coatings of  $\text{Cr}_3(\text{C}_{0.8}\text{N}_{0.2})_2$  have been deposited by combining a MOCVD process and an annealing post-treatment in the same reactor. The films were grown in the temperature range 410–520 °C by low pressure MOCVD using  $\text{Cr}(\text{NEt}_2)_4$  as single-source precursor. As-deposited films are very smooth and X-ray amorphous. A relatively low amount of nitrogen is uniformly incorporated into the films. The nitrogen content is nearly independent on the growth conditions and it amounts exactly the value required to form the metastable ternary phase ( $\sim 7$  at.%). As-deposited films crystallize upon annealing at 600 °C under vacuum to form the orthorhombic  $\text{Cr}_3(\text{C}_{0.8}\text{N}_{0.2})_2$  phase (Fig. 5). No evidence for additional phases has been found. Both as-deposited and annealed coatings exhibit a high hardness (17 GPa) and a good adhesion on stainless steel substrates [23].

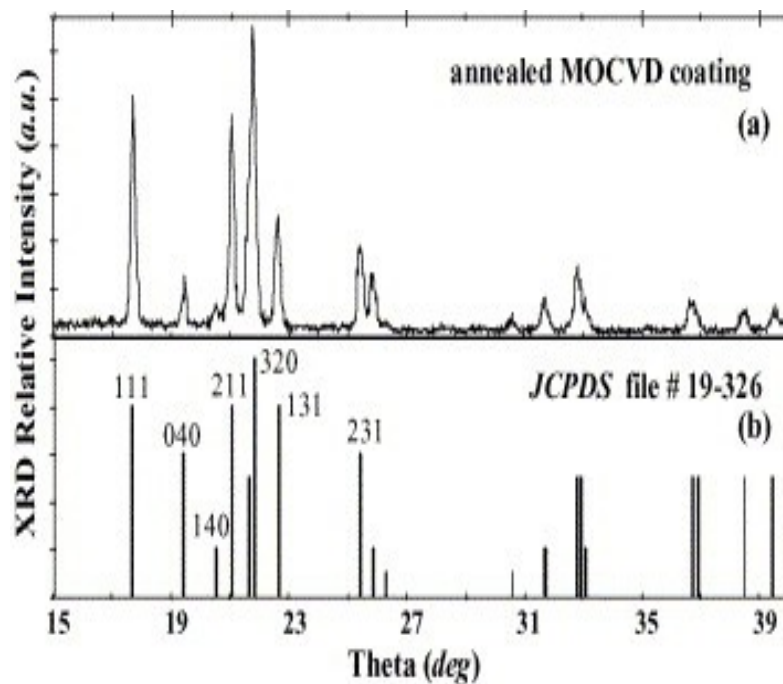


Fig. 5. Comparison of the XRD patterns of (a) an MOCVD  $\text{Cr}_3(\text{C}_{0.8}\text{N}_{0.2})_2$  coating after annealing at 600 °C under vacuum with (b) the JCPDS file of this ternary phase (nos. 19–326).

## 8. Conclusions

A series of MOCVD processes that permits the low temperature deposition of the stable and unstable solid phases of the Cr–C–N system have been presented. In agreement with partial

equilibrium calculations, the C content into the layers can be drastically reduced using the reactive gas mixture  $\text{BBCr}/\text{H}_2$  under atmospheric pressure and low  $x_{\text{BBCr}}$ . However, Cr metal is more conveniently deposited under low pressure using  $\text{BBCr}:\text{C}_6\text{Cl}_6$  gas mixtures. This process is kinetically controlled and a mechanism has been proposed. Chromium nitride coatings were produced at low temperature using the triple-source process  $\text{BBCr}:\text{C}_6\text{Cl}_6:\text{NH}_3$ . The C content of the layers is very low. Single phase CrN and dual phase  $\text{Cr}_2\text{N}:\text{CrN}$  coatings were deposited by controlling the input gas phase composition. Deposition of single phase  $\text{Cr}_2\text{N}$  coatings using this triple-source process will require only adjusting the  $\text{NH}_3:\text{BBCr}$  ratio keeping the other parameters constant. The use of these MOCVD processes for the growth of multilayer (superlattice) coatings such as those deposited by PVD, i.e. Cr/C [24], CrN/Cr [25], Cr/CrC [26] and CrN/NbN [24] is currently in progress.

### Acknowledgements

The author gratefully acknowledges Drs. C. Vahlas, L. Gueroudji, F. Ossola, F. Senocq and M. Nadal for their contribution to this research program.

### References

- J.-E. Sundgren and H.T.G. Hentzell, *J. Vac. Sci. Technol. A* 4 (1986), p. 2259.
- H. Holleck, *J. Vac. Sci. Technol. A* 4 (1986), p. 2661.
- F. Esaka, K. Furuya, H. Shimada, M. Imamura, N. Matsubayashi, H. Sato, A. Nishijima, A. Kawana, H. Ichimura and T. Kikuchi, *J. Vac. Sci. Technol. A* 15 (1997), p. 2521.
- G. Aldrich-Smith, D.G. Teer and P.A. Dearnley, *Surf. Coat. Technol.* 116–119 (1999), p. 1161.
- P. Engel, G. Schwarz and G.K. Wolf, *Surf. Coat. Technol.* 98 (1998), p. 1002.
- P. Hones, R. Sanjines and F. Levy, *Surf. Coat. Technol.* 94–95 (1997), p. 398.
- J.A. Sue and T.P. Chang, *Surf. Coat. Technol.* 76–77 (1995), p. 61.
- S.H. Yao and Y.L. Su, *Wear* 212 (1997), p. 85.
- J.F. Nowak, C. Duret-Thual, F. Maury, D. Oquab, Bull. Cercle Etudes Metaux, 15 (1987) 14.1.
- unha, M. Andritschky, L. Rebouta and K. Pischow, *Surf. Coat. Technol.* 116–119 (1999), p. 1152.
- M. Sikkens, A. Van Heereveld and E. Volgelzang, *Thin Solid Films* 108 (1983), p. 229.
- J.-C. Chuang, S.-L. Tu and M.-C. Chen, *J. Electrochem. Soc.* 146 (1999), p. 2643.
- S. Tsuboi, M. Seki, S. Kotsuji, T. Yoshihara, K. Fujii and K. Suzuki, *NEC Res. Dev.* 39 (1998), p. 127.
- P.M. Fabis, R.A. Cooke and S. McDonough, *J. Vac. Sci. Technol. A* 8 (1990), p. 3819.
- M. Taguchi and H. Takahashi, *J. Jpn. Inst. Met.* 56 (1992), p. 1221.
- J. Milosev and B. Navinsek, *J. Electrochem. Soc.* 140 (1993), p. L30.
- C. Vahlas, F. Maury and L. Gueroudji, *Adv. Mater. Chem. Vap. Deposition* 4 (1998), p. 69.
- F. Maury, C. Vahlas, S. Abisset and L. Gueroudji, *J. Electrochem. Soc.* 146 (1999), p. 3716.
- F. Schuster, F. Maury, J.F. Nowak and C. Bernard, *Surf. Coat. Technol.* 46 (1991), p. 275.
- R. Kieffer, P. Etmayer and T. Bubsy, *Z. Metallkde.* 58 (1967), p. 560.

F. Maury, D. Duminica and F. Senocq In: M.D. Allendorf and M.L. Hitchman, Editors, *Chem. Vap. Deposition XV. Electrochem. Soc. Proc. Vol., PV, 2000-13*, Electrochem. Soc., Pennington, NJ (2000), p. 260.

R. Sanjines, P. Hones and F. Levy, *Thin Solid Films* 332 (1998), p. 225.

F. Maury, F. Ossola and F. Senocq, *Surf. Coat. Technol.* 133–134 (2000), pp. 198–202

W.-D. Münz, *MRS Bulletin*, 28, March 2003, p. 173.

E. Martínez, J. Romero, A. Lousa and J. Esteve, *Surf. Coat. Technol.* 163–164 (2003), p. 571.

J. Romero, A. Lousa, E. Martínez and J. Esteve, *Surf. Coat. Technol.* 163–164 (2003), p. 392.

Tel.: +33 5 62 88 5669; fax: +33 5 62 88 5600.